Remote Sensing of Environment 115 (2011) 465–474

Contents lists available at ScienceDirect

Remote Sensing of Environment

journal homepage: www.elsevier.com/locate/rse

Quantification of aboveground rangeland productivity and anthropogenic degradation on the Arabian Peninsula using Landsat imagery and field inventory data

Katja Brinkmann [a,*], Uta Dickhoefer [b], Eva Schlecht [c], Andreas Buerkert [a]

[a] Organic Plant Production and Agroecosystems Research in the Tropics and Subtropics, University of Kassel, Witzenhausen, Germany
[b] Institute of Animal Nutrition and Physiology, Christian-Albrechts-Universität zu Kiel, Kiel, Germany
[c] Animal Husbandry in the Tropics and Subtropics, University of Kassel and Georg-August-Universität Göttingen, Germany

ARTICLE INFO

Article history:
Received 21 March 2010
Received in revised form 18 September 2010
Accepted 21 September 2010

Keywords:
Al Jabal al Akhdar
Allometric equations
ANPP modelling
NDVI trend analysis
Oman
Residual method
Semi-arid woodlands

ABSTRACT

The productivity of semi-arid rangelands on the Arabian Peninsula is spatially and temporally highly variable, and increasing grazing pressure as well as the likely effects of climatic change further threatens vegetation resources. Using the Al Jabal al Akhdar mountains in northern Oman as an example, our objectives were to analyse the availability and spatial distribution of aboveground net primary production (ANPP) and the extent and causes of vegetation changes during the last decades with a remote sensing approach. A combination of destructive and non-destructive biomass measurements by life-form specific allometric equations was used to identify the ANPP of the ground vegetation (<50 cm) and the leaf and twig biomass of phanerophytes. The ANPP differed significantly among the life forms and the different plant communities, and the biomass of the sparsely vegetated ground was more than 50 times lower (mean = 0.22 t DM ha^{-1}) than the biomass of phanerophytes (mean = 12.3 t DM ha^{-1}). Among the different vegetation indices calculated NDVI proved to be the best predictor for rangeland biomass.

Temporal trend analysis of Landsat satellite images from 1986 to 2009 was conducted using a pixel-based least square regression with the annual maximum Normalized Differenced Vegetation Index ($NDVI_{max}$) as a dependent variable. Additionally, linear relationships of $NDVI_{max}$ and annual rainfall along the time series were calculated. The extent of human-induced changes was analysed using the residual trends method. A strongly significant negative biomass trend detected for 83% of the study area reflected a decrease in annual rainfall but even without clear evidence of deforestation of trees and shrubs, human-induced vegetation degradation due to settlement activities were also important.

1. Introduction

In arid and semi-arid areas, rangelands play a vital role in the provision of forage for native and domestic herbivore animals, but they exhibit great temporal and spatial variation in aboveground net primary production (ANPP), reflecting differences in water availability and vegetation dynamics (Huenneke et al., 2002; McNaughton et al., 1989). Precipitation is one of the major driving forces for biomass availability in dry areas and is therefore highly correlated with vegetation cover, making semi-arid rangelands a sensitive indicator of climate change (Bai et al., 2004). In combination with increasing population and livestock pressure, climatic changes with a decline of precipitation can lead to land degradation, which is an increasing environmental problem on the Arabian Peninsula (Abahussain et al., 2002). For the Hajar Mountains of northern Oman, which provide important habitats for wildlife and endemic plant communities (Patzelt, in press), recent studies have shown that pasture areas near settlements are suffering from particularly strong degradation (Brinkmann et al., 2009; Patzelt, in press), whereby the amount and quality of fodder available for village-managed goat herds is diminishing (Schlecht et al., 2009). However, statistics on recent trends and the extent of land degradation on the Arabian Peninsula are still scarce (Abahussain et al., 2002) and monitoring tools are urgently needed to analyse the status and changes of rangeland vegetation. Since degradation is associated with a long-term decline in production, monitoring ANPP of rangeland vegetation is regarded as a valuable tool to indicate land degradation at different spatial and temporal scales (Diouf and Lambin, 2001; Prince et al., 1998; Tucker et al., 1991).

Different methods have been developed to estimate ANPP depending on the rate of biomass turnover of the ecosystem (Catchpole and Wheeler, 1992). As an alternative to labour and time intensive harvesting techniques, the 'double sampling procedure' uses a regression relationship of biomass to predictive variables, such as vegetation cover, plant height, leaf area or vegetation density (Cochran, 1977; Sala and Austin, 2000). Besides field measurements, applications based on satellite images for ANPP mapping and temporal change assessment

* Corresponding author. Fax: +49 5542 98 1230.
E-mail addresses: tropcrops@uni-kassel.de (K. Brinkmann and A. Buerkert), dickhoefer@aninut.uni-kiel.de (U. Dickhoefer), tropanimals@uni-kassel.de (E. Schlecht).

0034-4257/$ – see front matter
doi:10.1016/j.rse.2010.09.016

have been reviewed by several authors (Nemani et al., 2003; Tucker and Sellers, 1986). Numerous studies have shown that vegetation indices such as the Normalized Difference Vegetation Index (NDVI) can be strongly correlated with phytomass production in semi-arid areas (Diouf and Lambin, 2001) and is often used as a tool for detecting and quantifying large-scale changes in plant and ecosystem processes (Nemani et al., 2003; Tucker and Sellers, 1986; Wessels et al., 2007).

Because of the high inter-annual variability of climate in dry regions, any trend in NDVI over time is correlated with trends in climatic factors, especially precipitation (Tucker et al., 1991). Many studies have shown the dependence of vegetation on variations in rainfall and/or temperature. However, a major challenge in rangeland monitoring is the separation of climate effects from the effects of human activities (Evans and Geerken, 2004; Wellens, 1997; Wessels et al., 2007). Several studies proposed different techniques to identify anthropogenic land degradation using the Rain Use Efficiency (RUE; Diouf and Lambin, 2001; Prince et al., 1998; Wessels et al., 2007), or removing climate signals from NDVI time series by means of the RESTREND (Residual Trends) method (Archer, 2004; Evans and Geerken, 2004; Herrmann et al., 2005; Wessels et al., 2007). Once degradation trends have been identified with remote sensing techniques, the verification of the results poses a challenge, since there is often a lack of agreement on the existence and location of degraded land (Herrmann and Hutchinson, 2005; Prince et al., 1998). Most of the satellite-based time series analyses are based on the use of coarse spatial resolution information (NOAA/AVHRR satellites), limiting its usefulness for detailed studies in landscapes with important heterogeneity at finer scales (Belward and Lambin, 1990). Therefore in the present study medium-resolution Landsat satellite images were used to allow an appropriate spatial resolution that depicts the characteristics of the patchy vegetation cover of semi-arid rangelands. Taking the central Hajar Mountains of northern Oman as a case study for mountainous semi-arid rangelands, the objectives of this study were (i) to investigate the actual spatial distribution of ANPP and (ii) to analyse the extent and causes of vegetation changes during the last decades.

2. Materials and methods

2.1. Study area

The study was conducted on the central Al Jabal al Akhdar (23.07 N, 57.66 E; 400 km^2), a limestone massif characterised by a very rugged terrain with steep slopes within the Hajar mountain range of northern Oman. The local climatic conditions are arid to semi-arid, whereby rainfall ranges from 100 to 340 mm with an annual mean of 312 mm (Luedeling and Buerkert, 2008b). Approximately 54% of the rainfall occurs from January to April and 23% during July to August (Kwarteng et al., 2009) whereby the coefficient of variation in rainfall of a 48% reflects its high inter-annual variability (Fisher, 1994).

A dense network of dry riverbeds (in Arabic *wadi*) and small runnels, which remain relatively mesic for some time after a rainfall event, conveys drainage water north to the Batinah plain and south to the interior of Oman. The mountain rangelands have only sparse vegetation cover, largely limited to rills or small depressions where some sediments have accumulated in pockets. At higher altitudes (>1500 m a.s.l.) they are mainly characterised by semi-evergreen woodlands dominated by *Sideroxylon mascatense* together with *Dodonaea viscosa* and *Olea europaea* subsp. *cuspidata*, and above 2300 m a.s.l. by juniper (*Juniperus excelsa* subsp. *polycarpos*; Ghazanfar, 1991). Altogether, seven rangeland plant communities have been identified and mapped for this region, whereby the juniper woodlands (Teucrio–Juniperetum) are classified as a hotspot area for nature conservation (Brinkmann et al., 2009, 2010; Patzelt, in press).

The selected study area comprised the main local settlement, Sayh Qatanah, including 43 surrounding small settlements along an altitudinal range from 640 to 2560 m a.s.l. The oasis settlements receive their irrigation water for the cultivation of orchards and annual crops from permanent springs emerging from the limestone aquifers (Luedeling and Buerkert, 2008b). Grazing by goats and sheep as well as feral donkeys is the major anthropogenic impact on rangeland vegetation, apart from the ongoing urbanization process. The rangeland vegetation near the settlements provides over 50% of the daily feed intake of grazing goats, which is supplemented by feeds offered at the homestead (Dickhoefer et al., 2010; Schlecht et al., 2009).

2.2. Quantification of ANPP of herbaceous and ligneous species

A combination of destructive measurements and non-destructive approaches based on life-form specific allometric equations was used to quantify ANPP within an area of 100 km^2 near the central settlement of the Al Jabal al Akhdar plateau. For six plant communities most common on the studied rangelands (Teucrio–Juniperetum, Sideroxylon–Oleetum with a typical and a degraded variant, *Acacia gerrardii–Leucas inflata* community, *Ziziphus spina-christi–Nerium oleander* community, and *Moringa peregrina–Pteropyrum scoparium* community), we calculated the mean and standard deviation of the ANPP of ground vegetation and the leaf and twig biomass of phanerophytes, which were investigated as described below.

Using a systematic sampling design, the ANPP of the herbaceous[1] ground layer including all plants <0.5 m was recorded separately for grasses, forbs and sub-shrubs. All measurements were taken, in May 2009, four weeks after a rainfall event (>50 mm) at the peak of green biomass. At 105 sampling locations four frames of 1 m^2 each (total = 420) were placed at representative vegetation spots to measure the vegetation cover and mean plant height. Subsequently, the aboveground biomass was harvested 1 cm above the soil surface within 300 out of the 420 sampling frames. For each of the six plant communities common on the studied rangelands, 5–10 harvested samples separated by life form were taken and oven-dried (105 °C) to constant weight to determine biomass dry matter (DM). A multiple linear regression analysis was conducted to analyse the relationship among aboveground biomass DM, plant height and vegetation cover for each life form and to predict the aboveground biomass for the remaining 120 frames of which no destructive harvest was conducted. The biomass of the ground vegetation was then calculated as a mean for each sample location.

For the ANPP of phanerophytes (height > 0.5 m), we estimated the leaf and twig biomass using locally derived allometric equations established by Dickhoefer et al. (2010) for the most dominant tree and shrub species (*Olea europaea* L. ssp. *cuspidata* [Wall. ex G. Don] Ciferri, *Sideroxylon mascatense* [A. DC.] Penn., *Dodonaea viscosa* [L.] Jacq., *Euryops arabicus* Steud. ex Jaub. & Spach and *Sageretia thea* [Osb.] M.C. Johnst), and from literature for the *Ziziphus* (Cissé, 1980) and *Acacia* (Sanon et al., 2007) trees. All equations were based on the crown cover as an explanatory variable. Crown cover estimations and measurements of existing vegetation samples (n = 60) by Brinkmann et al. (2009) and biomass measurements (n = 5) by Dickhoefer et al. (2010) were used to calculate the species-specific leaf and twig biomass of shrubs and trees for the six plant communities. Since no allometric equations were available for *Juniperus excelsa* subsp. *polycarpos*, the leaf and twig biomass of phanerophytes within the Teucrio–Juniperetum in the upper north of the studied area was not modelled.

2.3. Remote sensing based spatial modelling of ANPP

Vegetation indices (VI) derived from satellite sensors were used to estimate the spatial and temporal distribution of vegetation biomass and annual ANPP. The NDVI is the ratio of the reflectance in the near-

[1] The term 'herbaceous' is used to denote all woody and non-woody plant species of the ground layer.

infrared (NIR) and red (RED) portions of the electromagnetic spectrum (Tucker, 1979), and is calculated as NDVI = (NIR − RED)/(NIR + RED). As the relationship between the NDVI and vegetation is known to be strongly affected by soil reflectance in sparsely vegetated areas of arid and semi-arid zones, the following additional vegetation indices were calculated for comparison:

- The Soil-Adjusted Vegetation Index (SAVI) proposed by Huete (1988), which minimizes the effects of soil background on the vegetation signal by incorporating a constant soil adjustment factor *L* into the denominator of the NDVI equation. We assumed *L* to equal 0.5, which was suggested by Huete (1988) for intermediate vegetation cover;
- The modified Soil-Adjusted Vegetation Indices (MSAVI) suggested by Qi et al. (1994), which is based on a modification of the *L* factor of the SAVI, which was derived by using the product of the NDVI and weighted difference vegetation index (WDVI). This index is based on the soil line concept, which describes the typical signatures of soils in a red/infrared bi-spectral plot and is obtained through linear regression of the near-infrared band against the red band for a sample of bare soil pixels.

The calculation of VIs was based on Landsat Level 1 terrain corrected images (L1T, resolution = 30 m) obtained from the US Geological Survey's Earth Resources Observation and Science (EROS). The L1T products already include radiometric, geographic and topographic corrections. The image data was recorded by the Enhanced Thematic Mapper Plus instrument (ETM+) at the same date of the biomass field survey during the peak vegetation growth to evaluate the relationship between imagery and field data. Since 2003, Landsat 7 imagery has been interrupted due to the failure of the Scan Line Corrector (SLC), which compensates for the forward motion of the satellite (Chander et al., 2009). As a result, each scene has data gaps. These were filled with the NASA gap filling tool "Frame and Fill" (NASA's Goddard Space Flight Center, Greenbelt, Maryland, USA) using two cloud-free Landsat 7 images of 30 April and 14 May 2009.

The at-sensor spectral radiance values of the Landsat data were converted to Top-Of-Atmosphere (TOA) reflectance values using the equations and parameters recommended by Chander et al. (2009). Reflectance values and VIs (NDVI, SAVI, and MSAVI) were calculated using the reflectance calculator and a graphical model in ERDAS Imagine 8.5 (Leica Geosystems GIS & Mapping LLC., Norcross, GA, USA). Relationships among VIs and recorded aboveground biomass were constructed using Ordinary Least Square regression (OSL) and Geographically Weighted Regression (GWR) within ArcGIS 9.3 (ESRI, Redlands, CA, USA). The latter allows the regression parameters and the strength of the relationship to vary over space by calculating the relationships separately for every data point or pixel. In contrast to global OSL, local GWR helps to overcome the problem of non-stationarity and reduces the problem of spatially autocorrelated error terms (Fotheringham et al., 2002). The corrected Akaike Information Criterion (AICc: Akaike, 1973) is used to compare the performance of the models with both OLS and GWR. The lower the AICc value the better will be the fit to the observed data. For each regression model, the Moran's *I* coefficient (Legendre and Legendre, 1998) was used as a measure of spatial autocorrelation to evaluate the pattern of the regression model residuals.

The best regression model was applied to predict the spatial distribution of ANPP using pixel-based regression analysis (Table 3). Due to the general weak correlation between ANPP of the herbaceous ground layer and VIs, we performed a spatial interpolation of the ANPP of the point sample location using the inverse distance weighting (IDW) methods.

2.4. Time series analysis of vegetation changes

Since the NDVI seemed to be the best predictor for the total biomass availability within the study area (Table 3), this index was subsequently used in order to detect and measure land degradation on rangelands and oasis agricultural lands of the study area. Long term changes of vegetation cover and production were analysed (400 km^2) using a series of Landsat satellite images (resolution = 30 m) from 1986 to 2009. For each year, 3–6 images (total = 59) of dates depicting the main growing season within each year were acquired (see supplementary data, Table 1). Unfortunately, only 0–2 usable Landsat images per year were available for the period 1989 to 1997. This was insufficient for an accurate cover of representative annual NDVI conditions; therefore these years were excluded from the time series.

For the SLC-off data from 2003 to 2009, we applied the gap filling procedure described in the previous section using fill scenes that were temporally close to the main scene (anchor) to minimize the effects of changing ground cover. Only cloud-free images of the study area were used and all images were converted to TOA reflectance, which provides better bases for comparison of data between images taken at different acquisition dates and/or by different sensors (Chander et al., 2009).

In order to eliminate the impact of bare soil, only NDVI values >0.05 were used in the trend analysis; all other values were set to zero. Furthermore, to maximize the range of values and provide numbers that are appropriate to display in an 8 bit image, the NDVI values were scaled as follows: $NDVI_{transformed} = 100\ (NDVI + 1)$. To smoothen the time series data, the highest $NDVI_{transformed}$ values for each pixel per year were calculated producing one singular Landsat $NDVI_{max}$ map for each year. This technique reduces atmospheric effects and minimizes sun-angle and shadow effects (Holben, 1986).

Temporal trend analysis was conducted as described by Archer (2004). On the basis of a pixel-based ordinary least squares (OLS) regression model ($Y = a + bx + \varepsilon$) the $NDVI_{max}$ was plotted as a function of time for each pixel of the dataset and the regression line was subsequently computed. The resulting image depicted the slope for each pixel's associated trend line and shows positive, stable or negative trends (Evans and Geerken, 2004). The significance level of these trends was analysed at a confidence level of 99% using t-tests.

2.5. Identification of climate and human-induced changes

To analyse the correlation between the trend in $NDVI_{max}$ and the trend in precipitation, rainfall data of the study area from the official weather station near Sayh Qatanah (World Meteorological Station No. 412540; 1950 m a.s.l.) were included. The daily rainfall records were obtained from the National Climatic Data Center (NCDC 2008) of the US National Oceanic and Atmospheric Administration (NOAA). A pixel-based linear regression analysis between $NDVI_{max}$ and the annual rainfall was conducted. Rainfall data was logarithmically transformed to fulfil the assumptions of normal distribution. To identify changes that are likely due to human degradation (grazing, firewood collection, and urbanization) the effects of precipitation were statistically removed by calculating for each pixel the difference between the observed $NDVI_{max}$ and the regression predicted $NDVI_{max}$, of the NDVI–rainfall relationship. This approach has been previously referred to as the RESTREND (Residual Tends) method (Archer, 2004; Evans and Geerken, 2004; Wessels et al., 2007), whereby the residuals (observed–predicted) were regressed on time and the significance was assessed using a t-test. Any trend through time present in the residuals should thus indicate changes in NDVI response not explained by rainfall effects (Evans and Geerken, 2004).

To compile the pixel results for the different land use and vegetation types separately, percentage of area, mean and standard deviation were calculated for six rangeland plant communities and oasis agricultural areas using an existing vegetation map of the study area (Brinkmann et al., 2010).

The areas where human degradation has occurred according to the results of the RESTREND method were visually inspected comparing a

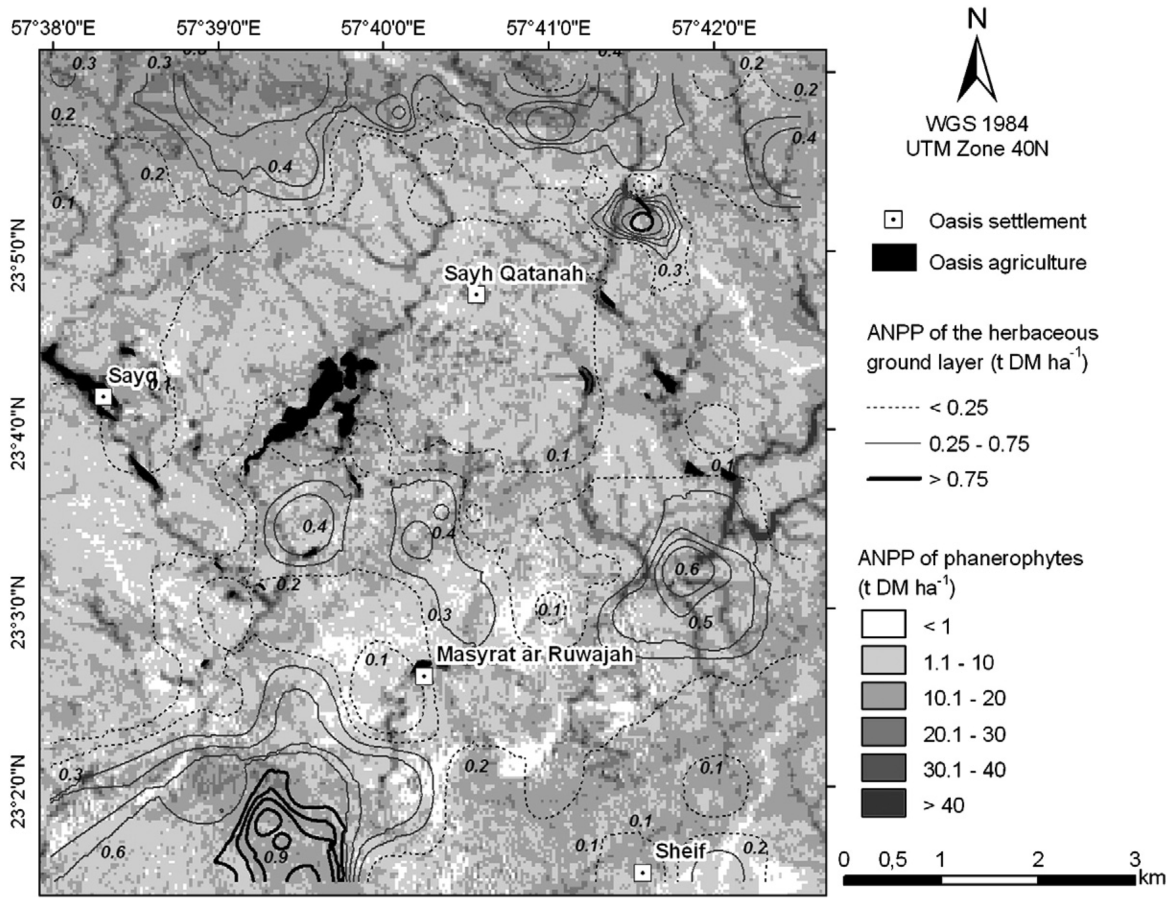

Fig. 1. Spatial distribution of the ANPP of phanerophytes (leaf and twig biomass, in t DM ha^{-1}) and the ANPP of the herbaceous ground layer (t DM ha^{-1}, shown by isolines) within a 100 km^2 rangeland area at Al Jabal al Akhdar (Oman) in spring 2009.

recent Google Earth® (Google, Mountain View, CA, USA) image of March 2009 with a high resolution Corona (KH-4B) scene from May 1972 and an aerial photograph from October 1992 (NSA/HLB, Al Dakhlyiah Oman Nr. 47 at the scale 1:50,000) obtained from the National Survey Authority of Oman.

3. Results

3.1. Quantification of ANPP of herbaceous and ligneous species

At the time of study, vegetation cover of the ground vegetation was on average only 4.1% with a mean height of 9 cm (Table 1). The total mean biomass production amounted to 21.2 DM g m^{-2} with a standard deviation of 18.7 g m^{-2}, reflecting the high spatial variability in biomass production of vegetated areas. Grasses and sub-shrubs dominated with a relatively high vegetation cover (0.5–25%) and biomass production (0.5–200 DM g m^{-2}).

Vegetation cover was a good predictor of biomass production for the three life forms as well as for total biomass estimation, with regression coefficients ranging from 0.65 to 0.74. Biomass height added little to the r^2 values except for grasses ($r = 0.26$). All the relationships between plant cover, height and biomass for the three life forms were significant ($p \leq 0.01$), whereby the coefficient of determination was higher for grasses than for forbs and sub-shrubs.

There were significant differences in herbaceous and ligneous biomass production among the six plant communities (Table 2). Overall, only 2% of the total ANPP was produced by the herbaceous ground layer (mean = 0.22 t DM ha^{-1}) and the mean ANPP of phanerophytes was 12.3 t DM ha^{-1}. ANPP was lowest for the degraded variant of the Sideroxylon–Oleetum, with a mean production of the ground vegetation of 0.12 t DM ha^{-1} (SD = 0.10) and a mean leaf and twig biomass of shrubs and trees of 4.5 t DM ha^{-1} (SD = 2.6). In contrast hereto, the productivity of the herbaceous ground layer, especially of grasses, was remarkably high for the typical variant of the Sideroxylon–Oleetum. Different peaks were

Table 1
Multiple linear regression coefficients, mean and standard deviation (SD) of the cover (%), dry matter (DM g m^{-2}) and height (cm) of 300 biomass samples (1 m^2) of the herbaceous ground layer collected on the Al Jabal al Akhdar (Oman) in spring 2009.

Species group	n	Beta		r^2	F-value	Cover (%)	Biomass (g m^{-2})	Height (cm)
		Cover	Height			Mean (SD)	Mean (SD)	Mean (SD)
Sub-shrubs	250	0.65	0.24	0.64	254.5	2.0 (1.3)	13.7 (12.8)	10.6 (7.7)
Grasses	290	0.74	0.26	0.81	703.2	2.6 (2.4)	12.8 (13.3)	8.3 (5.2)
Forbs	150	0.71	0.18	0.66	47.3	0.3 (0.3)	1.6 (2.2)	6.5 (6.3)
Total	300	0.65	0.33	0.77	173.3	4.1 (2.5)	21.2 (18.7)	9.1 (4.8)

Table 2
Area, mean and standard deviation (SD) of the annual net primary production (ANPP, t DM ha^{-1}) of the herbaceous ground layer and of phanerophytes (leaf and twig biomass) for the different plant communities within a 100 km^2 rangeland area at Al Jabal al Akhdar (Oman), as measured by field samples and life-form specific allometric equations.

Plant community	Area (km^2)	Herbaceous ground layer (t DM ha^{-1})			Phanerophytes (t DM ha^{-1})		
		n	Mean	SD	n	Mean	SD
Teucrio–Juniperetum	9.7	5	0.36	0.15	–	–	–
Sideroxylon–Oleetum (typical)	21.3	20	0.34	0.27	10	12.4	7.3
Sideroxylon–Oleetum (degraded)	36.3	49	0.12	0.10	15	4.5	2.6
Ziziphus spina-christi–Nerium oleander community	3.7	7	0.26	0.12	15	25.7	14.3
Acacia gerrardii–Leucas inflata community	20.5	16	0.28	0.21	15	10.1	8.5
Moringa peregrina–Pteropyrum scoparium community	8.5	8	0.24	0.20	10	7.2	5.6
Total	100	105	0.22	0.19	65	12.3	11.6

– Not measured.

detected for the ANPP of the herbaceous layer and the shrubs and trees of the six plant communities. Highest ANPP of phanerophytes was detected at temporally wet locations within the dry riverbeds characterised by the *Ziziphus spina-christi–Nerium oleander* community. At these locations the leaf and twig biomass amounted to 25 t DM ha^{-1} (SD = 14.3), whereas only little herbaceous biomass was found (mean = 0.26 t DM ha^{-1}). Rangelands of the Teucrio–Juniperetum also were sites with high herbaceous ANPP, which averaged 0.36 t DM ha^{-1}.

3.2. Spatial modelling of ANPP

For the rangelands of our study area, the peak NDVI was well below 0.7. In contrast to the leaf and twig biomass of phanerophytes, the correlations between the ANPP of the herbaceous ground layer and the vegetation index values were relatively low with coefficients ranging from 0.34 (MSAVI) to 0.47 (NDVI). The correlations of the modified vegetation indices (SAVI, MSAVI) with ANPP were generally lower than with the NDVI (Table 3). Overall, GWR revealed an improvement of the model performance for all predictor variables, which is evident from the higher coefficients of determination and AICc values. As expected, the error terms are most strongly autocorrelated for the global OLS models as indicated by Moran's *I*, whereas no significant positive autocorrelation was found for the GWR model residuals. The GWR model for ANPP of phanerophytes with NDVI as predictor variable had the best fit, with lowest AICc (417) and the highest R^2 (0.88) and was therefore used for the spatial prediction of ANPP (Fig. 1).

The interpolated biomass production of the herbaceous ground layer indicates two highly productive areas were grazing hardly occurs (peaks in Northeast and Southwest). The herbaceous layer is well developed at these sites with a productivity up to 1 t DM ha^{-1}, whereas the available ligneous biomass is undistinguished resulting in a total ANPP of 10–20 t DM ha^{-1}. Peaks of phanerophyte ANPP mainly occurred at wadi sites, runnels and in the north of the studied area. Total ANPP (<1 t DM ha^{-1}) was lowest near the central settlement Sayh Qatanah, along the roadside and at the steep slopes near the oasis Masayrat ar Ruwajah.

Table 3
Predictor variables (NDVI, SAVI, and MSAVI), Pearson correlation coefficient (R), corrected Akaike Information Criterion (AICc), coefficient of determination (R^2) and Moran's *I* autocorrelation coefficient of the ordinary least squares regression (OLS) and the geographically weighted regression (GWR) model for the annual net primary production (ANPP) of a 100 km^2 rangeland area at Al Jabal al Akhdar (Oman) in spring 2009.

Regression model	N	R	OLS			GWR		
			R^2	AICc	Moran's *I*	R^2	AICc	Moran's *I*
ANPP of phanerophytes								
NDVI	65	0.88	0.78	425	0.18*	0.88	417	0.11 n.s.
SAVI		0.87	0.76	432	0.23*	0.84	418	−0.04 n.s.
MSAVI		0.86	0.74	437	0.27*	0.85	420	−0.02 n.s.
ANPP of herbaceous ground layer								
NDVI	105	0.47	0.22	1501	0.42*	0.60	1467	0.05 n.s.
SAVI		0.37	0.14	1513	0.44*	0.60	1467	0.05 n.s.
MSAVI		0.34	0.12	1515	0.47*	0.60	1467	0.05 n.s.

n.s. = not significant (pattern is random); * = significant positive autocorrelation ($p \leq 0.001$).

3.3. Time series analysis of vegetation changes

Mean $NDVI_{max}$ fluctuations over time seemed similar for vegetation of rangelands and oasis agricultural areas, but the cultivated areas had in general a higher vegetation cover and density, resulting in higher mean $NDVI_{max}$ values (0.28 to 0.40; Fig. 2). For the rangelands $NDVI_{max}$ values were highest in 1988, 1998 and again in 2000. In the years preceding 2009, biomass tended to decline except for some increases in 2005 and 2007. For the rangeland areas as well as for the oasis agricultural areas, two ANPP minima were noted in 2002/2003 and 2008/2009.

Total rainfall tended to decline from 1986 to 2009. For the rangeland vegetation, highest $NDVI_{max}$ values corresponded to the wettest years of the time series. This suggests that the observed overall fluctuations in vegetation cover and density are mainly driven by changes in rainfall. In contrast, the relationship between high annual rainfall and high peak values of $NDVI_{max}$ was weaker for the irrigated agricultural areas, whereby $NDVI_{max}$ was highest in 1998.

For 1986–2009 a strongly significant total $NDVI_{max}$ decrease ($P \leq 0.01$) in 83% of the whole study area indicates a decline in ANPP for the majority of the rangeland communities (Table 4). However, these changes were different for the six plant communities and the agricultural areas. For the latter the decreasing trend was less pronounced and the majority of irrigated agricultural areas (69%) did not exhibit NDVI changes over the modelled period. The irrigated agricultural surface increased by 14%, mainly as a result of the establishment of an agricultural research area by the Ministry of Agriculture and Fisheries in 1992/93, and of a large private farm in 2001/2002. The surface dedicated to traditional oasis agriculture, in contrast, showed a decreasing trend during the indicated time period with old field terraces being abandoned.

3.4. Identification of climate and human-induced changes

Decreases in rangeland vegetation cover and ANPP as defined by significant trends of negative residuals indicating human-induced degradation were evident for the Teucrio–Juniperetum and the grazed variant of the Sideroxylon–Oleetum woodlands (Table 4). Together they comprised an area of 4 km^2. Nevertheless, over the study period the total human-induced changes in the study area seem relatively low. Only 1.4% of the total pixels showed strongly negative trends of residuals.

The Pearson correlation coefficient indicating the relationship between $NDVI_{max}$ and rainfall for the studied time period ranged from −0.6 to 0.82. The strongest relationship (mean r = 0.66; SD = 0.04) was found for the Teucrio–Juniperetum woodlands, whereas areas

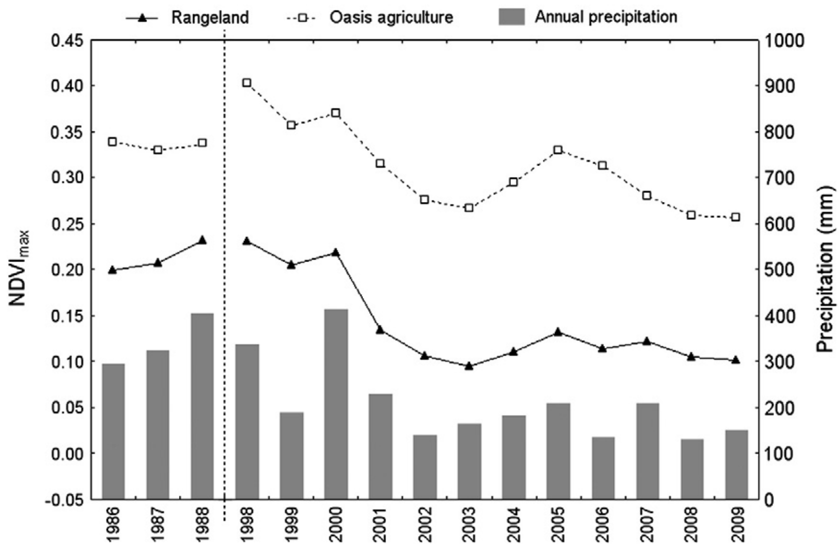

Fig. 2. Time sequence of mean $NDVI_{max}$ for the agricultural areas and the natural rangeland vegetation within the 400 km^2 study area at Al Jabal al Akhdar (Oman), and annual precipitation from 1986 to 2009. Each point represents the average $NDVI_{max}$.

receiving abundant run-off water had weaker rainfall–NDVI relationships, such as the *Ziziphus spina-christi–Nerium oleander* community with a mean correlation of $r=0.59$ ($SD=0.11$, Table 4). Pixels representing irrigated agricultural areas were with a mean correlation coefficient of $r=0.20$ ($SD=0.24$) only weakly correlated with rainfall.

Pixels with negative residual trends indicated areas where human-induced changes were expected (Fig. 3). Areas with negative trends of ANPP reflect mainly insufficient rainfall. However, in some parts, especially for the juniper woodlands in the north of the study area and for areas near the central settlement Sayh Qatanah, significant human-induced degradation was evident. Most apparent is the accumulation of these areas along the asphalted roads, which have been constructed from 2002 to 2006. Elsewhere there are some scattered pixels identifying ongoing degradation. Positive trends have been identified only for a small area (0.22 km^2) including a newly established private farm north of the road from Shnoot to Ar Roos.

4. Discussion

4.1. Herbaceous and ligneous ANPP

The biomass availability of different life forms (grasses, forbs, sub-shrubs, trees and shrubs) and plant communities at Al Jabal al Akhdar experienced a large variability in space and time. For the estimation of the ground vegetation, the vegetation cover was found to be the best predictor of biomass, which is in agreement with the findings of other studies (Andariese and Covington, 1986; Flombaum and Sala, 2007). Through the multiple linear regression approach using plant height as an additional predictor variable, the biomass of the ground vegetation could be reliably estimated and the results obtained correspond to earlier findings of Schlecht et al. (2009) and Dickhoefer et al. (2010).

Most of the species in the study area were woody perennials, which play a vital role for livestock nutrition (Dickhoefer et al., 2010; Schlecht et al., 2009). The determined ANPP of the herbaceous layer is similar to the average annual productivity of animal feed in the Arab regions of 0.28 t DM ha^{-1} mentioned by Abahussain et al. (2002). However, the data show that the biomass of the sparsely vegetated ground contributed little to the total ANPP. Lowest total ANPP was found for the degraded variant of the Sideroxylon–Oleetum, which is characterised by the highest browsing and grazing intensity at the Sayh Plateau (Brinkmann et al., 2009; Patzelt 2009). A comparison with studies from other semi-arid and arid ecosystems shows that the leaf and twig biomass of phanerophytes at Al Jabal al Akhdar was similar to that of the highlands of Ethiopia between 1500 and 2500 m a.s.l. (Mekuria et al., 2007), but higher than that of rangelands in the West African Sahel (Sanon et al., 2007).

Table 4
Areas that experienced a significant increase or decrease, no change, and human-induced degradation, as well as the mean and standard deviation (SD) of the pixel-based Pearson correlation between $NDVI_{max}$ and annual precipitation from 1986 to 2009 for oasis agriculture and rangeland plant communities in the 400 km^2 study area of the central Al Jabal al Akhdar (Oman).

	Area	Decrease ($P \le 0.01$)	No change	Increase ($P \le 0.01$)	Human degradation ($P \le 0.01$)	Response to rainfall (r)	
	km^2	%	%	%	km^2	Mean	SD
Oasis agriculture	1.6	22.8	69.1	14.0	<0.1	0.20	0.24
Rangeland plant communities:							
Teucrio–Juniperetum	85.3	92.8	7.3	0.0	2.1	0.66	0.04
Sideroxylon–Oleetum (typical)	107.0	80.5	19.5	0.0	0.3	0.63	0.06
Sideroxylon–Oleetum (degraded)	63.1	94.9	6.2	0.0	1.8	0.64	0.05
Ziziphus spina-christi–Nerium oleander community	10.8	56.0	41.1	0.0	0.3	0.59	0.11
Acacia gerrardii–Leucas inflata community	80.1	77.8	23.2	0.0	0.7	0.61	0.08
Moringa peregrina–Pteropyrum scoparium community	52.1	76.6	24.4	0.0	0.5	0.61	0.09
Total	400	83.8	16.3	<0.1	5.8	0.63	0.07

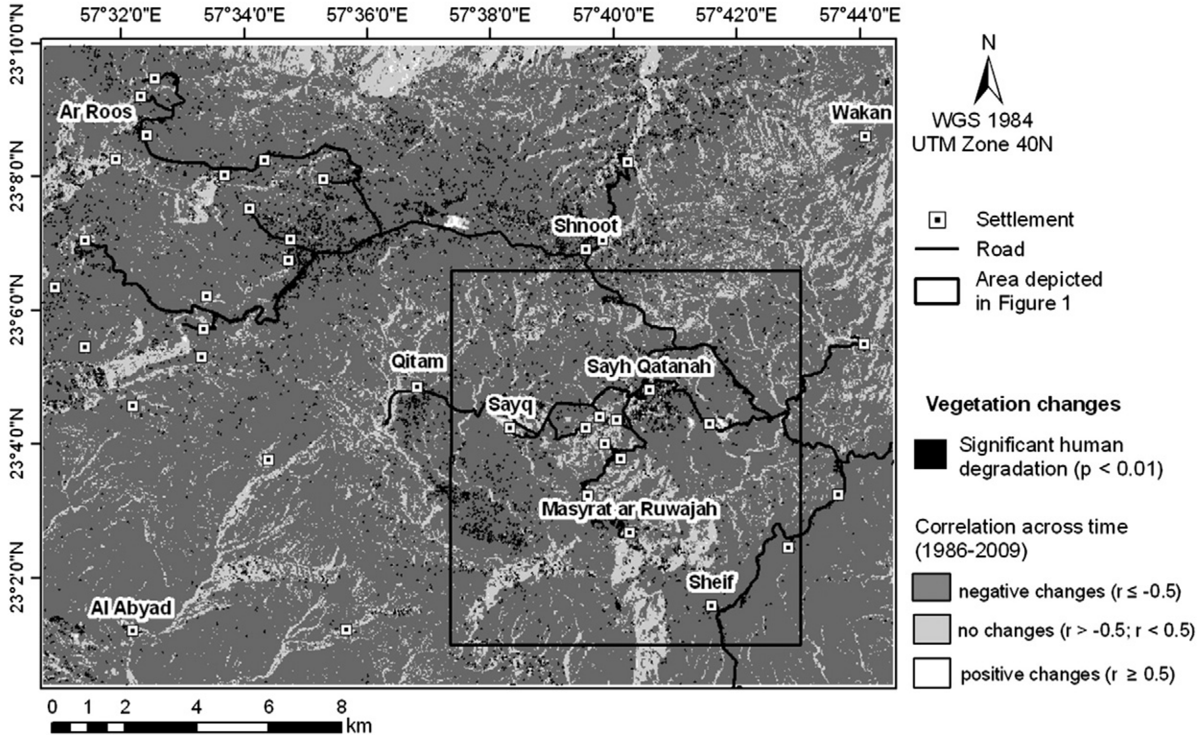

Fig. 3. Spatial representation of vegetation changes showing pixels of significant human degradation ($p<0.01$) and the correlation of pixel-specific $NDVI_{max}$ values across time (1986–2009) with negative changes ($r\leq-0.5$), no changes ($r>-0.5$ and <0.5) and positive changes ($r\geq0.5$) within the 400 km^2 study area on the central Al Jabal al Akhdar (Oman).

Many arid landscapes are characterised by source–sink systems, where plant productivity is largely dependent on surface run-off from bare areas to vegetated patches (HilleRisLambers et al., 2001). This typically results in a mosaic or pattern composed of patches with high vegetation density alternating with patches of a low-cover or bare soil component (Barbier et al., 2006; Lejeune et al., 2004). In our study area ANPP of trees and shrubs was generally higher at wadi sites, which are characterised by the *Ziziphus spina-christi–Nerium oleander* community, compared to non-wadi sites with a mean crown cover of 44% (maximum = 80%), whereas on plateau sites the crown cover was less than 18% (Brinkmann et al., 2009). Fisher and Gardner (1995) reported for the juniper woodlands similar results, whereby trees in the wadi habitat were both taller and in better condition than trees outside the wadi habitat. As a result of higher vegetation density the leaf and twig biomass of the *Ziziphus spina-christi–Nerium oleander* community was generally more than two times higher than in other rangeland communities (Dickhoefer et al., 2010).

4.2. Spatial modelling of ANPP

Accurate image-based monitoring of ANPP in semi-arid areas is often limited by the effects of bare soil, vegetation clumping and the resulting non-linear relationships between measured signals and the biophysical properties of the vegetation (Huete et al., 1992). However, our field measurements revealed that the performance of ANPP prediction of SAVI and MSAVI, which were developed specifically to help account for the effects of background soil reflectance in such areas (Huete, 1988; Qi et al., 1994), was not higher compared to NDVI. This might be explained by the estimated soil line parameters for MSAVI, which were not substantially different from that assumed by the NDVI in the present study area.

In contrast to the foliar biomass of phanerophytes, the SAVI, MSAVI, and NDVI were poor predictors for the biomass of ground vegetation. This was most likely due to the presence of senescent or dry vegetation, especially at ungrazed sites, where the ANPP of the ground vegetation was generally higher. The sparse vegetation cover in general and the overshading by the trees and shrubs may also have contributed to errors. It is known that non-photosynthetically active vegetation exhibits elevated visible reflectance which hampers the use of indices that rely on the ratio between visible and mid-infrared reflectance patterns (Todd et al., 1998). In semi-arid rangelands, herbaceous vegetation that remains dry or senescent for the majority of the year may still provide valuable forage. Hence, different methods have been tested to account for the non-photosynthetically active vegetation such as the Relative Spectral Mixture Analysis (RSMA; Okin, 2007), the Normalized Difference Senescent Vegetation Index (NDSVI; Qi et al., 2002) or the Soil-Adjusted Total Vegetation Index (SATVI, Marsett et al., 2006), which is based on the NDSVI. The latter was tested in the current study and its applicability seems limited to the estimation of the total ANPP, since the overshading effects of trees and shrubs remain still problematic if someone wants to differentiate between the (understorey) herbaceous and ligneous biomass. The use of the SATVI also requires a meaningful separation between green and senescent biomass during field survey to successfully calibrate and interpret the results of this index (Marsett et al., 2006).

Nevertheless the NDVI approach of the present study provided a reasonable estimate for the leaf and twig biomass of phanerophytes, which represents 98% of total ANPP in the study region and can thus be used for predictive mapping. The modelled ANPP map revealed different spatial peaks of herbaceous and ligneous biomass. Highest biomass of the herbaceous ground layer was concentrated in small areas where grazing hardly occurs. One is an enclosure of the Agricultural Research Centre near Sayh Qatanah that was fenced off 15 years ago. The other area, situated on a plateau at Ras al Kabul, is very difficult to access and therefore grazing by either domestic goats or feral donkeys rarely occurs, leaving the vegetation relatively undisturbed. The leaf and twig biomass of phanerophytes, however, was highest along the wadi sites and in the north of the study area within the Teucrio–Juniperetum. However, the potential biomass productivity of this community may be substantially higher, since it has its ecological optimum above

2200 m a.s.l. and was not well represented (n = 5) within the 100 km^2 sampling grid studied here. Destructive field measurements were impossible for the dominating tree species, since the *Juniperus excelsa* M. Bieb. subsp. *polycarpos* (K.Koch) Takhtajan was classified as a vulnerable species (Patzelt, 2007) and is therefore strongly protected from cutting. Its real leaf and twig biomass may therefore be underestimated.

4.3. Time series analysis of NDVI

Total biomass significantly declined along the time series in 83% of the pixels investigated, which was mainly triggered by lower annual rainfall (<250 mm) during that period. Based on the identified NDVI–ANPP relationships total ANPP was estimated to have been twice as high in 1986–1988 as compared to 2009. Semi-arid vegetation is known to respond to changing rainfall conditions rather fast, but there may be a carry-over or lag-effect of extended dry or wet periods on vegetation growth in subsequent seasons (Wiegand et al., 2004). In their analysis of Oman's rainfall data Kwarteng et al. (2009) observed no major periods of drought and no significant changes in precipitation trends during 1977–2003, but they reported high rainfall for 1995–1998, when all meteorological stations in Oman recorded above-average precipitation. This time span was not completely covered here, but the likely carry-over effects of the wet years were visible (Fig. 3).

The rainfall–NDVI relationship differed in strength for the different vegetation types (Table 4), but the decline in ANPP was remarkably similar (Fig. 3). For eight years annual rainfall was far below the 312 mm long-term average reported by Fisher (1994). However, the same author also indicated that drought periods lasting at least two subsequent years with annual rainfall <100 mm are common. Brook and Sheen (2000) detected apparent 5-year cycles of rainfall in Oman and the United Arab Emirates. Since 2001 annual rainfall never exceeded the mean and for the Muscat region a negative rainfall trend has been identified, in which the period 1997–2006 had the lowest decadal rainfall record since 1974 (Kotwicki and Al Sulaimani, 2009).

The high correlation (mean r = 0.63) between annual rainfall and $NDVI_{max}$ is comparable to values reported elsewhere in semi-arid regions (Diouf and Lambin, 2001; Prince et al., 1998; Wessels et al., 2007). For our correlation analysis rainfall data from an official weather station at Sayh was used which, unfortunately, contained some data gaps over the period covered by our time series analysis. A comparison with our own precipitation measurements from 2007 to 2009 revealed a failure in the station's rain gauge measurements during June 2007, when Oman was hit by the tropical cyclone Gonu. The corresponding heavy rainfalls have not been recorded by the meteorological station at Sayh and the annual rainfall data was therefore corrected using our own measurements (Dickhoefer et al., 2010). Further corrections using additional rainfall data from other, nearby stations such as the one from Nizwa (800 m a.s.l.) were not feasible, since the data of the lowlands was not representative for the mountainous rangeland area studied here. Despite further possible gaps in rainfall data, the detected NDVI fluctuations along the time series fit quite well into the annual rainfall pattern for the study period.

Most of the studies on NDVI trends are focusing on relatively large scales using low resolution, high temporal frequency satellite data (NOAA/AVHRR satellites) with a limited explanatory power for changes at smaller scale. For a detailed site specific rangeland monitoring, the medium-resolution Landsat data set is more accurate. However, Landsat 7 images pose a disadvantage for trend analysis due to the long return time, cloud, haze and the SLC-failure since 2003 (Chander et al., 2009). The latter requires cumbersome post-processing of data using 1–2 temporally near satellite scenes to fill the gaps of one image. A main problem is thus the acquisition of enough suitable scenes to depict the seasonal and/or annual vegetation conditions for a valid comparison along the time series. The SLC-off effects are most pronounced along the edge of the scene and gradually diminish towards the centre of the scene, whereby the middle of the scene (ca. 22 km wide) contains very little duplication or data loss (Chander et al., 2009). Since our analysed study area was situated near the centre of the images (0–10 km), the NASA gap filling tool resulted in reasonably seamless image products. However, reliable gap filling is more problematic and an appropriate trend observation might be unfeasible near the edge of the Landsat scene.

4.4. Human-induced land degradation

A promising technique for removing the masking effects of the rainfall–NDVI relationship is the pixel-based RESTREND method, also successfully applied by Archer (2004), Evans and Geerken (2004) and Wessels et al. (2007). The latter authors discussed the major weaknesses of this method, but also stressed its usefulness to monitor green biomass trends and conditions of rangeland vegetation triggered by effects other than rainfall. The trend in the residuals is strongly affected by the point in the time series when degradation has taken place, whereby degradation that has occurred in the first or last years of the time series would be difficult to detect (Wessels et al., 2007). If there is an influence of any causative variables other than rainfall, which had been left out in the regression model, residuals are assumed to contain substantial amounts of noise (Herrmann et al., 2005). The inclusion of household based livestock data as another predictor variable in the regression model used would probably indicate more specific human-induced changes in terms of grazing intensity. However, yearly statistics on the household or village based livestock data that covers the whole time frame are unavailable for the study area.

Using NPP as an indicator is another quantitative approach to identify the role of human activities on degradation. Xu et al. (2009) modelled the potential NPP (determined by climatic conditions without human disturbances) and the difference between the potential and actual NPP to measure the impacts of climate change and human activities on degradation, respectively. However, the model scale is so coarse that it is not often applied at finer scales.

Independently from the statistical method used, there are also some degradation factors that could not be identified properly using a single satellite-based approach, such as species impoverishment with a replacement of palatable species by non-palatable ones with little or no change in green biomass. Yet overall, the RESTREND method delivers valuable indications of areas that are subjected to particularly strong human-induced changes. Once identified they can be investigated in more detail using field measurements or high resolution satellite images (Evans and Geerken, 2004; Wessels et al., 2007). The verification of the present results by site inspections showed that areas with a predicted significant human-induced degradation corresponded to actually degraded areas (see supplementary data, Fig. 1). However, only human disturbances resulting in sizeable vegetation change could be traced through the Landsat datasets; similar to the study of Evans and Geerken (2004), isolated small-scale changes triggered by overgrazing or firewood collection were not visible. Degradation in form of newly established residential areas of the central settlement Sayh Qatanah, which included a larger but fragmented area of irrigated home gardens were not accurately recognized due to the only local increase of NDVI values over the time series of the images analysed.

The rapid social and infrastructural development which has thoroughly transformed the Sultanate of Oman since the beginning of the political opening and commercial oil exploitation in the early 1970s has also affected the traditional landuse systems at Al Jabal al Akhdar. The identified anthropogenic degradation in the study area covered a total of 6 km^2 and resulted from the construction of roads, residential, governmental and military areas. Until 2000, public access to the study area was restricted. In 1998, a network of gravel roads was established and the urbanization of the Sayh Plateau began. To date the town of Sayh Qatanah covers an area of about 500 ha and is projected to double its size within the next few years (Dickhoefer et al., 2010). About seven additional settlements have been established in the period from 1986 to 2009. On the other hand, one third of the original area of old terrace land has been gradually abandoned, reportedly as a result of the farmer-perceived increasing shortage of water (Luedeling and Buerkert, 2008a) and labour scarcity induced by alternative income opportunities (Dickhoefer et al., 2010). Archaeological evidence shows that relatively intense pastoral and sedentary grazing systems have a century-old tradition in the study region (Schreiber, 2007). Thus, most of the detected larger anthropogenic disturbances from 1986 to 2009 resulting in a significant loss of vegetation cover cannot be explicitly attributed to deforestation or overgrazing.

5. Conclusions

The status and changes of semi-arid rangeland vegetation in rugged mountains can only be monitored systematically and regularly from satellite remote sensing platforms. However, for the low productive herbaceous layer with a large amount of senescent standing litter the NDVI, SAVI and MSAVI were unsuitable to estimate ANPP. Thus, further remote sensing indices and techniques need to be tested for forage assessment in semi-arid areas, which take into account the proportion of photosynthetically inactive vegetation, whereby field measurements should separate between green and senescent biomass components.

For rangeland monitoring techniques a particular challenge is the capacity to distinguish between natural and anthropogenic impacts. Using medium-resolution Landsat images, the residual trend method provides valuable hints for rangeland monitoring on potential human-induced degraded areas, but it should be combined with a detailed analysis of the degraded areas using high resolution satellite data and/or statistics and reports on land use activities, livestock and population numbers. Without clear evidence of massive deforestation of trees and shrubs, ongoing human-induced degradation at Al Jabal al Akhdar seems mainly due to urbanization. Our results revealed an area between Shnoot and Wakan in the north of the study area within the *Juniperus* woodlands (Teucrio–Juniperetum), which was nearly undisturbed since 1986. As large parts of the area in which *Juniperus* occurs in Oman have already been identified as a potential National Scenic Reserve, this undisturbed area can be recommended for conservation within the framework of the planned nature reserve designation.

Acknowledgements

The authors are grateful to Bernd Brinkmann for his technical support and to Muhammed Al Rawahi for his logistical help during the field survey. We thank the Agricultural Service at Sayh Qatanah for good cooperation, and the German Research Foundation (DFG) for funding (BU 1308). We also gratefully acknowledge the patience and hospitality of the oasis farmers of Al Jabal al Akhdar.

Appendix A. Supplementary data

Supplementary data to this article can be found online at doi: 10.1016/j.rse.2010.09.016.

References

Abahussain, A. A., Abdu, A. S., Al-Zubari, W. K., El-Deen, N. A., & Abdul-Raheem, M. (2002). Desertification in the Arab Region: Analysis of current status and trends. *Journal of Arid Environments*, *51*, 521−545.

Akaike, H. (1973). Information theory and an extension of the maximum likelihood principle. In B. N. Petrov, & N. Caski (Eds.), *Proceedings of the Second International Symposium on Information Theory* (pp. 267−281). Budapest: Akademiai Kiado.

Andariese, S. W., & Covington, W. W. (1986). Biomass estimation for four common grass species in Northern Arizona Ponderosa Pine. *Journal of Rangeland Management*, *39*, 472−473.

Archer, E. R. M. (2004). Beyond the "climate versus grazing" impasse: Using remote sensing to investigate the effects of grazing system choice on vegetation cover in the eastern Karoo. *Journal of Arid Environments*, *57*, 381−408.

Bai, Y. F., Han, X. G., Wu, J. G., Chen, Z. H., & Li, L. H. (2004). Ecosystem stability and compensatory effects in the Inner Mongolia grassland. *Nature*, *431*, 181−184.

Barbier, N., Couteron, P., Lejoly, J., Deblauwe, V., & Lejeune, O. (2006). Self-organized vegetation pattering as a fingerprint of climate and human impact on semi-arid ecosystems. *Journal of Ecology*, *94*, 537−547.

Belward, A., & Lambin, E. F. (1990). Limitations to the identification of spatial structures from AVHRR data. *International Journal of Remote Sensing*, *11*, 921−927.

Brinkmann, K., Patzelt, A., Dickhoefer, U., Schlecht, E., & Buerkert, A. (2009). Vegetation patterns and diversity along an altitudinal and a grazing gradient in the Jabal al Akhdar mountain range of northern Oman. *Journal of Arid Environments*, *73*, 1035−1045.

Brinkmann, K., Patzelt, A., Schlecht, E., & Buerkert, A. (2010). Use of environmental predictors for vegetation mapping in semi-arid mountain rangelands and the determination of conservation hotspots. *Journal of Applied Vegetation Science*. doi:10.1111/j.1654-109X.2010.01097.x.

Brook, G. A., & Sheen, S. -W. (2000). Rainfall in Oman and the United Arab Emirates: Cyclicity, influence of the southern oscillation, and what the future may hold. *The Arab World Geographer*, *3*, 78−96.

Catchpole, W. R., & Wheeler, C. J. (1992). Estimating plant biomass: A review of techniques. *Australian Journal of Ecology*, *17*, 121−131.

Chander, G., Markham, B. L., & Helder, D. L. (2009). Summary of current radiometric calibration coefficients for Landsat MSS, TM, ETM+, and EO-1 ALI sensors. *Remote Sensing of Environment*, *113*, 893−903.

Cissé, M. I. (1980). The browse production of some trees of the Sahel: Relationships between maximum foliage biomass and various physical parameters. In H. N. Le Houérou (Ed.), *Browse in Africa: The current state of knowledge* (pp. 204−208). Addis Ababa: ILCA.

Cochran, W. G. (1977). *Sampling techniques* (3rd ed.). New York: John Wiley & Sons.

Dickhoefer, U., Buerkert, A., Brinkmann, K., & Schlecht, E. (2010). The role of pasture management for sustainable livestock production in semi-arid subtropical mountain regions. *Journal of Arid Environments*, *74*, 962−972.

Diouf, A., & Lambin, E. F. (2001). Monitoring land-cover changes in semi-arid regions: Remote sensing data and field observations in the Ferlo, Senegal. *Journal of Arid Environments*, *48*, 129−148.

Evans, J., & Geerken, R. (2004). Discrimination between climate and human-induced dryland degradation. *Journal of Arid Environments*, *57*, 535−554.

Fisher, M. (1994). Another look at the variability of desert climates, using examples from Oman. *Global Ecology and Biogeography Letters*, *4*, 79−87.

Fisher, M., & Gardner, A. S. (1995). The status and ecology of a *Juniperus excelsa* subsp. *polycarpos* woodland in the northern mountains of Oman. *Vegetatio*, *119*, 33−51.

Flombaum, P., & Sala, O. E. (2007). A non-destructive and rapid method to estimate biomass and aboveground net primary production in arid environments. *Journal of Arid Environments*, *69*, 352−358.

Fotheringham, A. S., Brunsdon, C., & Charlton, M. (2002). *Geographically weighted regression: The analysis of spatially varying relationships.* Chichester: Willey.

Ghazanfar, S. A. (1991). Vegetation structure and phytogeography of Jabal Shams, an arid mountain in Oman. *Journal of Biogeography*, *18*, 299−309.

Herrmann, S. M., Anyambab, A., & Tucker, C. T. (2005). Recent trends in vegetation dynamics in the African Sahel and their relationship to climate. *Global Environmental Change*, *15*, 394−404.

Herrmann, S. M., & Hutchinson, C. F. (2005). The changing context of the desertification debate. *Journal of Arid Environments*, *63*, 538−555.

HilleRisLambers, R., Rietkerk, M., van den Bosch, F., Prins, H. H. T., & de Kroon, H. (2001). Vegetation pattern formation in semi-arid grazing systems. *Ecology*, *82*, 50−61.

Holben, B. N. (1986). Characteristics of maximum-value composite images from temporal AVHRR data. *International Journal of Remote Sensing*, *7*, 1417−1434.

Huenneke, L. F., Anderson, J. P., Remmenga, M., & Schlesinger, W. H. (2002). Desertification alters patterns of aboveground net primary production in Chihuahuan ecosystems. *Global Change Biology*, *8*, 247−264.

Huete, A. R. (1988). A soil-adjusted vegetation index (SAVI). *Remote Sensing of Environment*, *83*, 195−213.

Huete, A. R., Hua, G., Qi, J., Chehbouni, A., & van Leeuwen, W. J. D. G. (1992). Normalization of multidirectional red and NIR reflectances with the SAVI. *Remote Sensing of Environment*, *41*, 143−154.

Kotwicki, V., & Al Sulaimani, Z. (2009). Climates of the Arabian Peninsula — Past, present, future. *International Journal of Climate Change Strategies and Management*, *1*, 297−310.

Kwarteng, A. Y., Dorvlo, A. S., & Kumar, G. T. V. (2009). Analysis of a 27-year rainfall data (1977–2003) in the Sultanate of Oman. *International Journal of Climatology*, *29*, 605−617.

Legendre, P., & Legendre, P. (1998). *Numerical ecology* (2rd ed.). Amsterdam: Elsevier Science.

Lejeune, O., Tlidi, M., & Lefever, R. (2004). Vegetation spots and stripes: Dissipative structures in arid landscapes. *International Journal of Quantum Chemistry*, *98*, 261−271.

Luedeling, E., & Buerkert, A. (2008a). Effects of land use changes on the hydrological of mountain oases in northern Oman. *Plant and Soil*, *304*, 1−20.

Luedeling, E., & Buerkert, A. (2008b). Typology of oases in northern Oman based on Landsat and SRTM imagery and geological survey data. *Remote Sensing of Environment*, *112*, 1181−1195.

Marsett, R. C., Qi, J., Heilman, P., Biedenbender, S. H., Watson, M. C., Amer, S., et al. (2006). Remote sensing for grassland management in the arid Southwest. *Rangeland Ecology & Management*, *59*, 530−540.

McNaughton, S. J., Oesterheld, M., Frank, D. A., & Williams, K. J. (1989). Ecosystem-level patterns of primary productivity and herbivory in terrestrial habitats. *Nature*, *341*, 142−144.

Mekuria, W., Veldkamp, E., Haile, M., Nyssen, J., Muys, B., & Gebrehiwot, K. (2007). Effectiveness of exclosures to restore degraded soils as a result of overgrazing in Tigray, Ethiopia. *Journal of Arid Environments*, *69*, 270−284.

Nemani, R. R., Keeling, C. D., Hashimoto, H., Jolly, W. M., Piper, S. C., Tucker, C. J., et al. (2003). Climate-driven increases in global terrestrial net primary production from 1982–1999. *Science*, *300*, 1560−1563.

Okin, G. S. (2007). Relative spectral mixture analysis — A multitemporal index of total vegetation cover. *Remote Sensing of Environment*, *106*, 467−479.

Patzelt, A. (2007). *Oman plant red data book. The office of the advisor for conservation of the environment.* Muscat: Diwan of Royal Court, Sultanate of Oman.

Patzelt, A. in press. The mountain vegetation of northern Oman: Ecology, phytosociology and biogeography of *Olea europaea* and *Juniperus excelsa* woodlands and of weed vegetation on cultivated terraces. In R. Victor, & M. Robinson (Ed.), Al Jabal Al Akhdar Monograph, Muscat, Sultanate of Oman.

Prince, S. D., Brown de Colstoun, E., & Kravitz, L. (1998). Evidence from rain use efficiencies does not support extensive Sahelian desertification. *Global Change Biology*, *4*, 359−374.

Qi, J., Chehbouni, A., Huete, A. R., Kerr, Y. H., & Sorooshian, S. (1994). A modified soil adjusted vegetation index (MSAVI). *Remote Sensing of Environment*, *48*, 119−126.

Qi, J., Marsett, R., Heilman, P., Biedenbender, S., Moran, M. S., Goodrich, D. C., et al. (2002). RANGES improves satellite-based information and land cover assessments in Southwest United States, EOS transactions. *American Geophysical Union*, *83*, 601−606.

Sala, O. E., & Austin, A. T. (2000). Methods of estimating aboveground net primary productivity. In O. E. Sala, R. B. Jackson, H. A. Mooney, & R. W. Howarth (Eds.), *Methods in Ecosystem Science* (pp. 31−43). New York, Berlin, Heidelberg: Springer.

Sanon, H. O., Kaboré-Zoungrana, C., & Ledin, I. (2007). Edible biomass production from some important browse species in the Sahelian zone of West Africa. *Journal of Arid Environments*, *71*, 376−392.

Schlecht, E., Dickhoefer, U., Gumpertsberger, E., & Buerkert, A. (2009). Grazing itineraries and forage selection of goats on mountainous rangelands in the Al-Jabal-al-Akhdar massive, Oman. *Journal of Arid Environments*, *73*, 355−363.

Schreiber, J. (2007). Transformationsprozesse in Oasensiedlungen Omans. Die vorislamische Zeit am Beispiel von Izki, Nizwa und dem Jebel Akhdar. Thesis, Ludwig-Maximilians-Universität, Munich.

Todd, S. W., Hoffer, R. M., & Milchunas, D. G. (1998). Biomass estimation on grazed and ungrazed rangelands using spectral indices. *International Journal of Remote Sensing*, *19*, 427−438.

Tucker, C. J. (1979). Red and photographic infrared linear combinations for monitoring vegetation. *Remote Sensing of Environment*, *8*, 127−150.

Tucker, C. J., Dregne, H. E., & Newcomb, W. W. (1991). Expansion and contraction of the Sahara Desert from 1980 to 1990. *Science*, *253*, 299−301.

Tucker, C. J., & Sellers, P. J. (1986). Satellite remote-sensing of primary production. *International Journal of Remote Sensing*, *7*, 1395−1416.

Wellens, J. (1997). Rangeland vegetation dynamics and moisture availability in Tunesia: An investigation using satellite and meteorological data. *Journal of Biogeography*, *24*, 845−855.

Wessels, K. J., Prince, S. D., Malherbe, J., Small, J., Frost, P. E., & VanZyl, D. (2007). Can human-induced land degradation be distinguished from the effects of rainfall variability? A case study in South Africa. *Journal of Arid Environments*, *68*, 271−297.

Wiegand, T., Snyman, H. A., Kellner, K., & Paruelo, J. M. (2004). Do grasslands have a memory: Modeling phytomass production of a semiarid South African grassland. *Ecosystems*, *7*, 243−258.

Xu, D. Y., Kang, X. W., Zhuang, D. F., & Pan, J. J. (2009). Multi-scale quantitative assessment of the relative roles of climate change and human activities in desertification — A case study of the Ordos Plateau, China. *Journal of Arid Environments*, *74*, 498−507.